Vol 17 No 12, December 2008
1674-1056/2008/17(12)/4428-06

Chinese Physics B

© 2008 Chin. Phys. Soc.
and IOP Publishing Ltd

The chaotic property in the autoionization of Rydberg lithium atom*

Zhou Hui(周 慧), Li Hong-Yun(李洪云), Gao Song(高 嵩),
Zhang Yan-Hui(张延惠), Jia Zheng-Mao(贾正茂), and Lin Sheng-Lu(林圣路)†

College of Physics and Electronics, Shandong Normal University, Jinan 250014, *China*

(Received 6 March 2008; revised manuscript received 8 April 2008)

This paper presents theoretical computations of the ionization rate of Rydberg lithium atom above the classical ionization threshold using semiclassical approximation. The yielded random pulse trains of the escape electrons are recorded as a function of emission time such that they can be related to the terms of the recurrence periods of the photoabsorption. This fact illustrates that it is ionic core scattering processes which give rise to chaos in autoionization dynamics and this is verified by comparison of our results with the hydrogen atom situation. In order to reveal the chaotic properties in detail, the sensitive dependence of the ionization rate upon the scaled energy is discussed for different scaled energies. This approach provides a simple explanation for the chaotic character in autoionization decay of Rydberg alkali–metal atoms.

Keywords: chaos, autoionization, semiclassical theory, core scattering
PACC: 0545, 3280D, 0365S, 3260S

1. Introduction

The autoionization phenomena of the highly excited Rydberg atoms in external fields have been studied extensively over the past decade. Most experimental studies on the ionization dynamics focused on the recurrences of alkali–metal atoms in an electric field excited above the classical ionization threshold.[1−3] In 1996, Noordam *et al* studied autoionization of rubidium atom in a static electric field of 2.0 kV/cm at scaled energy $\varepsilon = -1.54$ by experiment, in which rubidium atom was excited from the ground state to an energy above the classical saddle point by a short (few picoseconds) laser pulse. The resulting electron flux striking a detector was then measured as a function of emission time. This ionization signal revealed a random train of electron pulses, rather than an exponential decay as believed previously.[4] In 2003, Mitchell and Delos theoretically discussed the escape rates of hydrogen atom in external fields by using semiclassical method.[5] In the following year, they illustrated the transport and escape mechanism concerning to the chaos-induced pulse trains in the ionization of hydrogen atom by a homoclinic tangle technique.[6]

However, the theoretical description of the autoionization property of non-hydrogen atom in external fields is not well developed. Some works[7−9] have declared that the ionic core induces important effects which cannot be seen in hydrogen atom, whereas the quantitative connection between the recurrence and autoionization is still obscure. In this paper, we present theoretical computations of the ionization rate of lithium atom in an applied electric field, and analyse the structure of the pulse trains of the emitting electrons. In contrast to the Rydberg hydrogen atom, where the pulses of the emission electrons are caused by applied external magnetic field, while at present the pulse trains for lithium atom case are created through core scattering. Using semiclassical method, we achieve a simple yet obvious improvement understanding the autoionization property. This work provides a quasi-quantitative explanation for raising the complicated chaotic behaviour. And the conclusions can be directly compared with those of hydrogen atom as well as the future experimental results.

2. Theoretical computations of the ionization rate

The Hamiltonian of lithium atom in an applied electric field directed along the z axis is given in cylin-

*Project supported by the National Natural Science Foundation of China (Grant Nos 10774093 and 10374061).
†Corresponding author. E-mail: sllin@sdnu.edu.cn

drical coordinates (ρ, z) and atomic units ($e \equiv \hbar \equiv m = 1$) by

$$H = \frac{1}{2}\left(P_z^2 + P_\rho^2\right) + V(\rho, z) + Fz, \tag{1}$$

where F is the electric field strength and the model potential $V(\rho, z)$ has the explicit form,[8]

$$\begin{aligned} & V(\rho, z) \\ = & V_{\text{Coulomb}}(\rho, z) + V_{\text{core}}(\rho, z) \\ = & -\frac{1}{\left(\rho^2 + z^2\right)^{1/2}} - \frac{Z-1}{\left(\rho^2 + z^2\right)^{1/2}} \\ & \times \left(1 + \frac{\left(\rho^2 + z^2\right)^{1/2}}{a}\right)\left\{\exp\left[\frac{-\left(\rho^2 + z^2\right)^{1/2}}{a}\right]\right\} \end{aligned} \tag{2}$$

with Z the atomic number and a the parameter of the model potential, which is chosen to give the measured quantum defect. For the case of lithium, $Z = 3$, the optimized value of the parameter is given by $a = 1/2.13$.[10]

As is common,[11] we transform the original variables to the scaled ones $\tilde{r} = rF^{1/2}, \tilde{P} = PF^{-1/4}, \tilde{t} = tF^{3/4}, \varepsilon = EF^{-1/2}$ and the effective Planck constant $\hbar_{\text{eff}} = F^{1/4}$, then the classical motion is governed by the scaled Hamiltonian

$$\begin{aligned} \tilde{H} = & HF^{1/2} \\ = & \frac{1}{2}\left(\tilde{P}_\rho^2 + \tilde{P}_z^2\right) - \frac{1}{\left(\tilde{\rho}^2 + \tilde{z}^2\right)^{1/2}} \\ & - \frac{Z-1}{\left(\tilde{\rho}^2 + \tilde{z}^2\right)^{1/2}}\left(1 + \frac{\left(\tilde{\rho}^2 + \tilde{z}^2\right)^{1/2}}{a}\right) \\ & \times \left\{\exp\left[\frac{-\left(\tilde{\rho}^2 + \tilde{z}^2\right)^{1/2}}{a}\right]\right\} + \tilde{z}. \end{aligned} \tag{3}$$

Strictly speaking, the scaled law is not available for multi-electron atom due to the existence of the ionic core. However, in semiclassical scheme the classical limit only is valid far away from the nucleus one might ignore the small inner region near the nucleus, thus the scaled property is still a good approximation for non-hydrogen atom under consideration here. From Eq.(3), we find that the scaled Hamiltonian does not depend on the energy E and electric field strength F separately but only on the scaled energy $\varepsilon = EF^{-1/2}$.

In order to eliminate the Coulomb singularity in the Hamiltonian which is important in describing the motion of the electron wave packet, following standard practice,[12] we introduce semi-parabolic coordinates, (u, v)

$$u = (\tilde{r} + \tilde{z})^{1/2}, v = (\tilde{r} - \tilde{z})^{1/2}, \tag{4}$$

$$p_u = \tilde{p}_\rho v + \tilde{p}_z u,$$

$$p_v = \tilde{p}_\rho u - \tilde{p}_z v, \quad \frac{\mathrm{d}\tilde{t}}{\mathrm{d}\tau} = u^2 + v^2, \tag{5}$$

where τ is the scaled time and its scaled unit equals 52 picoseconds in a static electric field of 19 V/cm in this paper. Moreover, the angle θ between the z axis and the trajectory in cylindrical coordinates is twice the value of the angle Θ between the u axis and the trajectory in parabolic coordinates.

We define an effective Hamiltonian $h = 2\tilde{r}(\tilde{H} - \varepsilon)$,

$$\begin{aligned} & h(u, v, p_u, p_v) \\ = & \frac{1}{2}\left(p_u^2 + p_v^2\right) + V_{uv}(u, v) - 2, \end{aligned} \tag{6}$$

$$\begin{aligned} V_{uv} = & -\varepsilon\left(u^2 + v^2\right) + \frac{1}{2}\left(u^4 - v^4\right) \\ & -4\left\{\exp\left[\frac{-\left(u^2 + v^2\right)}{2a}\right]\right\}. \end{aligned} \tag{7}$$

Using a short laser pulse we can excite the ground state or low-energy state s electron of a lithium atom to an energy above the classical saddle point, $E_c = -2\sqrt{F}$, where F is the applied static electric field. In the scaled variables, the scaled energy $\varepsilon = E/\sqrt{F}$, $\varepsilon = 0$ stands for the zero field ionization limit and $\varepsilon = -2$ is the so-called classical ionization threshold or classical saddle point energy. Considering the define bandwidth of the short laser pulse, we find that a coherent superposition of several Stark states is excited, creating an outgoing radial wave packet in all directions which consists of the initial outgoing Coulomb wave[9]

$$\begin{aligned} & \Phi_0(r_0, \theta_i^j) \\ = & -\mathrm{i}\pi^{1/2} 2^{3/4} r_0^{-3/4} \mathrm{e}^{\mathrm{i}(\sqrt{8r_0} - 3\pi/4)} y(\theta_i^j), \end{aligned} \tag{8}$$

where $y(\theta)$ is the angular distribution.

Because the radially outgoing wave far away from the nucleus can be expressed by an ensemble of classical trajectories, we calculate the ionization rate by integrating an initial ensemble of radial outgoing trajectories with a single fixed scaled energy $\varepsilon = -1.3$ and precise launch time $t = 0$ from the core to the position $\tilde{z} = -4$, where the detector is located. The total number of trajectories striking the detector per unit time (i.e. the ionization rate) is then recorded as a function of time. The ionized electron flux gives rise to a pulse train seen in the detector plane, which

is shown in Fig.1(a). Figure 1(b) shows the time taking a trajectory (with fixed energy $\varepsilon = -1.3$) to strike the detector as a function of its initial launched angle θ. The dashed lines connect the escape segments (i.e. icicles[13]) in Fig.1(b) to their corresponding pulses in Fig.1(a). Each peak conforming to an escape segment (icicle) implies that a different ensemble of electron trajectories reached the detector at different time intervals: for example, the trajectory which heads directly downhill ($\theta = \pi$) reaches the detector first. As θ decreases, the initial velocity is further and further away from the downhill direction, and the trajectory takes longer and longer time to reach the detector. Eventually a critical angle θ_c is achieved, at which the trajectory takes an infinite time to escape. This trajectory is bounded forever. The ionization curve with exponential tail in Fig.1(a) is also equal to the slope $\mathrm{d}\theta/\mathrm{d}t$ of the escape-time plotted in Fig.1(b), weighted by the initial angular distribution $|y(\theta)|^2 \sin\theta$. The angular distribution is an s wave, and we choose the angular distribution $|y(\theta)|^2 = 1$ for theoretical convenience, since it weights all directions evenly. Following Ref.[13], we use the term 'icicle' standing for the pulse in Fig.1(a) that starts at the earliest escape time in Fig.1(b) and then trails off to zero as θ approaches the critical angle and $\mathrm{d}\theta/\mathrm{d}t$ goes to zero.

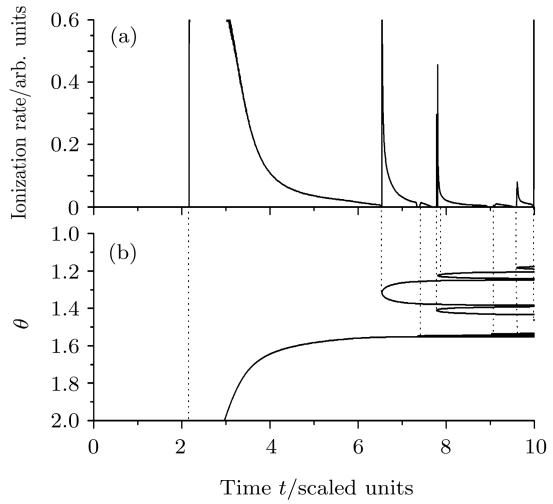


Fig.1. (a) The ionization rate for lithium atom above the classical saddle point with $\varepsilon = -1.3$, $N = 80$ and $F = 19\,\mathrm{V/cm}$ is plotted as a function of time after atomic excitation. (b) The time taking a trajectory to strike the detector is plotted as a function of the initial launch angle θ.

3. Results and discussions

Exploring classical escape dynamics requires a detailed understanding of the structure of the electron pulse train in escape-time plot. At first glance, it is completely random either in the pulse strength or in the pulse pattern. The fact that the peak-to-peak spacing is roughly the recurrence time hints strongly that the autoionization mechanism should be intimately related to the closed orbit with multiple core scattering.

In order to show the important role of core scattering in raising chaos, we draw the ionization rate curve of hydrogen under identical conditions in Fig.2.[6] We can see distinctly from the case of lithium that there stands only a single electron pulse in Fig.2(a). Consequently, in Fig.2(b), only one critical angle appears. These results are expectable since pure Coulomb scattering does not bring about any chaotic behaviour and there is no chaos for Rydberg hydrogen in an external electric field, only one electron pulse decayed at exponential rate is reasonable.

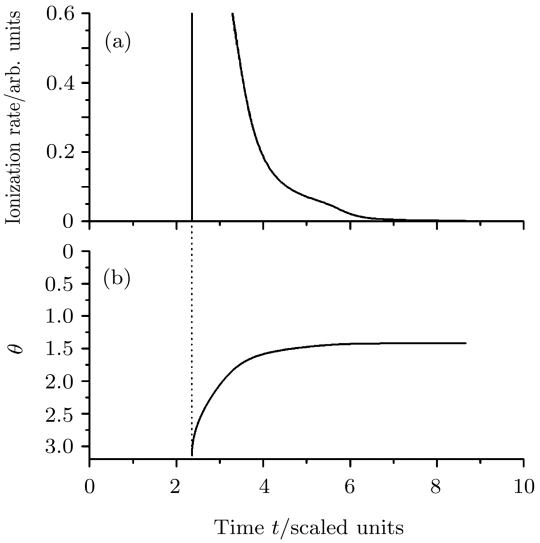


Fig.2. (a) The ionization rate is plotted as a function of time after atomic excitation for hydrogen atom in an electric field, with the scaled energy $\varepsilon = -1.3$, $N = 80$ and $F = 19\,\mathrm{V/cm}$. (b) The time taking a trajectory to strike the detector is plotted as a function of the initial launched angle θ.

These distinct phenomena can be qualitatively explained by the semiclassical analysis. After the atom-exciting part of the wave packet slipping over the classical barrier is drawn downhill by the applied electric field and strikes the detector which measures the ionization rate as a function of time, the rest which either initially heads uphill or has larger launched angles than the critical angle θ_c is turned around by the field, a fraction of which returns to the core where it is scattered in all directions, and that part which

fortunately heads downhill creates a second pulse of electrons. Subsequent multiple non-Coulomb scattering events create additional more complicated pulses.

We examine in detail peak–peak spacing in an escape-time plot and reveal that it is coincident with the recurrence period of Rydberg lithium in the same conditions.[14] Some shorter closed orbits that stand for the central trajectory of the electron wave packet are displayed in Fig.3(a), (b), (c) in the semi-parabolic coordinates, their scaled recurrence times are 1.45, 4.36, 3.77 and their initial launched angle θ are 0.0, 1.31, 1.55, respectively. Figure 3(d) shows the directly downhill trajectory which takes the scaled time of 2.162 to strike the detector. Therefore, the corresponding angle Θ in Fig.3 are 0.0, 1.57, 0.66, and 0.78, respectively.

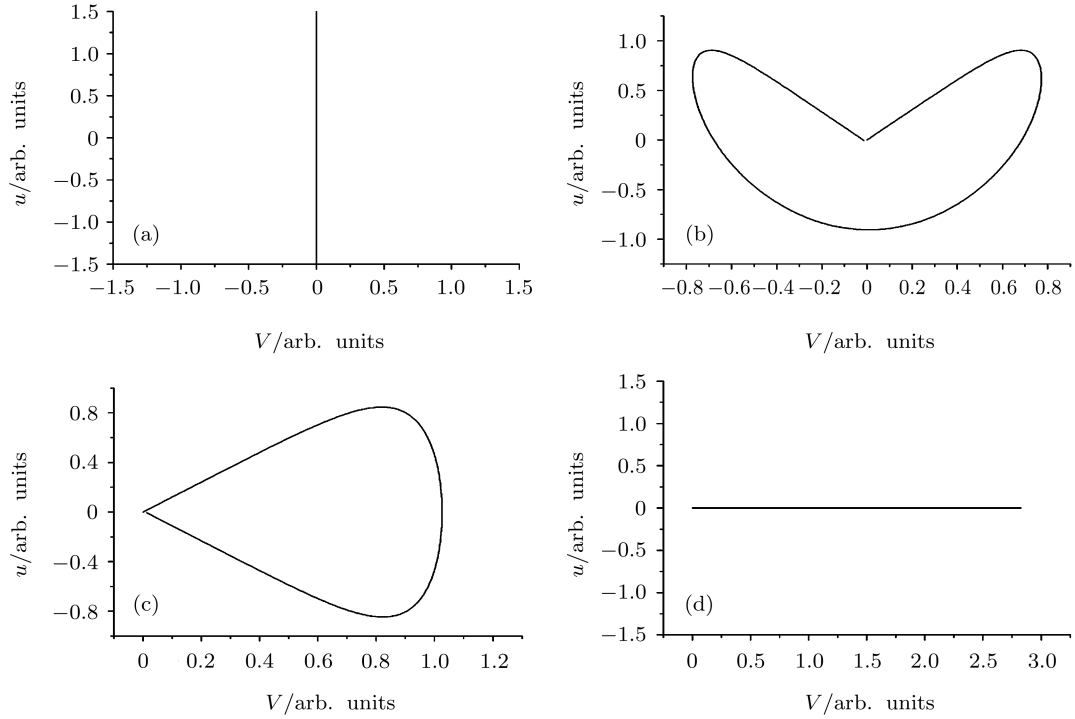


Fig.3. (a), (b), (c) depict some closed orbits which stand for the central trajectory of the ensemble of the electron trajectories. And (d) presents the directly downhill trajectory in the semi-parabolic coordinates, where $\varepsilon = -1.3$, $N = 80$, $F = 19\,\mathrm{V/cm}$.

The explicit comparison is as follows: the first pulse in Fig.1 is the initial prompt pulse induced by the electron trajectories heading directly downhill and reaching detect plane. The other pulses could be attributed to the contribution of some combinatorial closed trajectories arisen from the core scattering. For example, the forepart of the second pulse begins at the scaled time of 6.54, which can be considered as the fact that the electron first travels along the closed orbit in Fig.3(b) and then is scattered to the direct downhill trajectory in Fig.3(d) through core scattering. Similarly, the origination of the third peak at scaled time of 7.38 can be seen as the sum of two core scattering from the closed orbits in Figs.3(a) to (c) and then enters directly downhill trajectory in Fig.3(d). Other pulses can be analysed in the same way.

In the framework of semiclassical theory, the scaled energy dominates the dynamic behaviour of the system particularly for the irregular motion in the chaotic region. Any small variation of the scaled energy will dramatically affect the state of the initial outgoing electron wave packet including its initial launched angle and velocity, thus might significantly alter the shape of the closed orbit and consequently notably change its recurrence time and recurrence strength. So we calculate the ionization rate of lithium at scaled energy $\varepsilon = -1.4$ and $\varepsilon = -1.2$, and the results are presented in Figs.4(a) and 5(a) respectively, while the corresponding escape time as a function of the initial launched angle θ is shown in Figs.4(b) and 5(b). For the sake of conciseness, we only list part of the results of earlier time here.

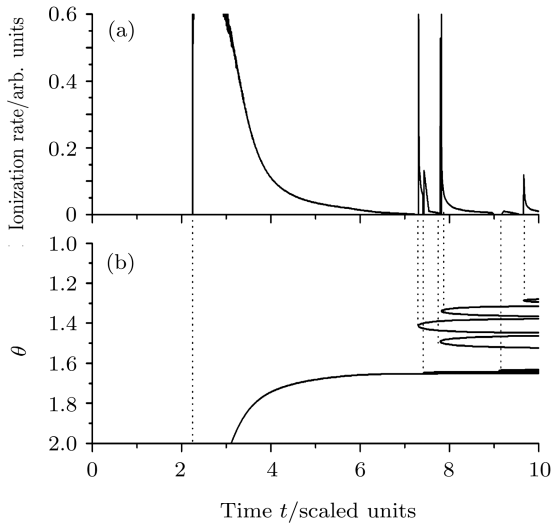


Fig.4. (a) The ionization rate of lithium atom in an applied electric field with $\varepsilon = -1.4$ is plotted as a function of time after atomic excitation. (b) The time taking a trajectory to strike the detector is plotted as a function of the initial launched angle θ.

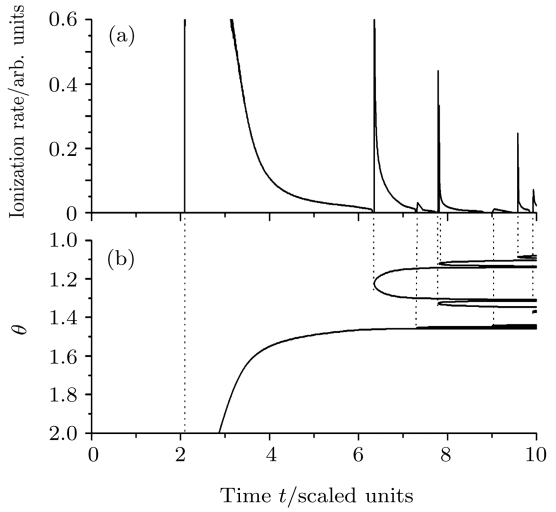


Fig.5. (a) The ionization rate for lithium atom in an applied electric field with $\varepsilon = -1.2$ is plotted as a function of time after atomic excitation. (b) The time taking a trajectory to strike the detector is plotted as a function of the initial launched angle θ.

Comparing Fig.1(a) with Figs.4(a) and 5(a), we can easily see that the lower the scaled energy is, the later every electron pulse begins. It is easy to understand the underlying physical reason for this: as the energy decreases, the time required by a trajectory from origin to the detector becomes longer. Also, both the pattern and the strength of each corresponding peak in these figures are completely different, which reveal chaos depending sensitively on the initial conditions. Examining Figs.1(b), 4(b) and 5(b), we find that the value of corresponding critical angle significantly decreases with the increase of energy, which can be explained by the fact that the smaller the launched angle is, the more energy it requires for the trajectory to turn backward to strike the detector.

4. Conclusion

By using semiclassical method, we theoretically computed the ionization rate of lithium atom in an electric field at the scaled energy $\varepsilon = -1.2$, $\varepsilon = -1.3$ and $\varepsilon = -1.4$, which are all above the classical saddle point value $\varepsilon = -2$, and also discussed the dynamical behaviour. The results reveal that the chaotic property of lithium atom is reflected in the structure of the electron pulse trains and measured as functions of electronic emitting time and the initial launched angle, which can be explained in terms of the recurrence periods through multiple core scattering, therefore, indicate that under suitable energy and external fields two kinds of different dynamic processes, autoionization and recurrence, are related each other. This work provides a quantitative elucidation for the complicated chaotic property in autoionization of the Rydberg nonhydrogen atoms. In this paper we concentrate our attention on the classical density of electron flux without taking the interference between electron pulses into account. For shorter time and sufficiently high excitation (large N), it should yield a reasonable approximation to the intensity seen at the detector plane. The investigation would also provide a convenient laboratory tool for studying chaotic transport and escape.

References

[1] Broers B, Christian J F, Hoogenraad J H, van der Zande W J, van Linden van den Heuvell H B and Noordam L D 1993 *Phys. Rev. Lett.* **71** 344

[2] Broers B, Christian J F and van Linden, van den Heuvell H B 1994 *Phys. Rev.* A **49** 2498

[3] Lankhuijzen G M and Noordam L D 1995 *Phys. Rev.* A **52** 2016

[4] Lankhuijzen G M and Noordam L D 1996 *Phys. Rev. Lett.* **76** 1748

[5] Mitchell A, Handley J P, Tighe B and Delos J B 2003 *Chaos* **13** 880

Mitchell A, Handley J P, Tighe B and Delos J B 2003 *Chaos* **13** 892

[6] Mitchell K A, Handley J P, Tighe B and Delos J B 2004 *Phys. Rev. Lett.* **92** 073001

Mitchell K A, Handley J P, Tighe B and Delos J B 2004 *Phys. Rev.* A **70** 043407

[7] Gao J and Delos J B 1992 *Phys. Rev.* A **46** 1449

[8] Hüpper B, Main J and Wunner G 1996 *Phys. Rev.* A **53** 744

[9] Dando P A, Monteiro T S, Delande D and Taylor K T 1996 *Phys. Rev.* A **54** 127

[10] Courtney M, Spellmeyer N, Jiao H and Kleppner D 1995 *Phys. Rev.* A **51** 3604

[11] Delande D and Buchleitner A 1994 *Advances in Atomic Molecular and Optical Physics* **34** 85

[12] Song X H and Lin S L 2003 *Acta Phys. Sin.* **52** 1611 (in Chinese)

[13] Tiyapan A and Jaffé C 1995 *J. Chem. Phys.* **103** 5499

[14] Du M L and Delos J B 1988 *Phys. Rev.* A **38** 1896

Du M L and Delos J B 1988 *Phys. Rev.* A **38** 1913